NATIONAL AERONAUTICS AND SPACE ADMINISTRATION

Technical Report 32-1336

Improving Biomedical Image Quality With Computers

Robert H. Selzer

JET PROPULSION LABORATORY
CALIFORNIA INSTITUTE OF TECHNOLOGY
PASADENA, CALIFORNIA

October 1, 1968

NATIONAL AERONAUTICS AND SPACE ADMINISTRATION

Technical Report 32-1336

Improving Biomedical Image Quality With Computers

Robert H. Selzer

JET PROPULSION LABORATORY
CALIFORNIA INSTITUTE OF TECHNOLOGY
PASADENA, CALIFORNIA

October 1, 1968

TECHNICAL REPORT 32-1336

Prepared Under Contract No. NAS 7-100
National Aeronautics & Space Administration

Preface

The work described in this report was performed by the Space Sciences Division of the Jet Propulsion Laboratory.

PRECEDING PAGE BLANK NOT FILMED.

Contents

Figures

Contents (contd)

Figures (contd)

Abstract

The analysis of pictorial data in the biomedical fields has increased sufficiently in the past few years to warrant the use of computers to process this data. A description of image processing research conducted at the Jet Propulsion Laboratory, particularly in the area of image enhancement, is contained in this paper. Frequency-response methods, which allow computer processing techniques to be directly related to the imaging system and to the image subject, are discussed. The most important enhancement technique, two-dimensional digital filtering, is described and illustrated with numerical examples. Examples of before-and-after computer-processed pictures are shown which illustrate low-pass, high-pass, high-frequency restoration, feature-selective and nonlinear filters. Subtraction techniques are also discussed and an example is given of a computerized film-measurement procedure that requires preprocessing of the image by filtering techniques. This application involves measurement of the width of trabecular bone shadows from x-ray film.

Improving Biomedical Image Quality With Computers

I. Importance of Image Processing

Pictorial data has long been an important source of information in medicine and biology, but until quite recently, little use has been made of computers to process this data. Perhaps the major obstacle to such development was the difficulty of getting pictures into and out of the computer. The character recognition systems developed in the fifties were, in general, not applicable to biomedical image problems because of the restrictive nature of the input devices. High resolution image scanners with the ability to detect multiple shades of grey were required and, while such devices became available in the early sixties, it was difficult to find biomedical applications that would justify their cost which frequently fell into the half-million dollar range.

In the past two or three years the cost of scanners has gone down and the need for image processing has gone up. As a result, the prospects are quite good that computers will be used extensively within the next two to five years both for image enhancement and for pictorial data-extraction. Some of the current and potential areas of application are described in the following paragraphs.

When used to enhance existing pictures, the computer is potentially capable of producing an absolute improvement in image quality because processing methods are available that can retrieve information partially lost in the image generating system. These techniques are applicable to x-ray films, to photomicrographs, or to virtually any type of photographic data.

The computer can also remove useless data or emphasize selected classes of features. Processing of this type might be used for mass screening of medical x-ray film in the hope of reducing viewing time. Considering the fact that over 200 million x-ray films were made in the United States last year, it is clear that computer-aided analysis of radiographs is a useful objective.

The current interest in computer image processing has been intensified by the recent emergence of biomedical techniques that require objects on film to be counted or measured. Computer methods have already been extensively applied to the problem of counting and sorting human chromosomes (karyotyping). As an example, one film-scanning system karyotypes a cell in 20 seconds —

an activity that requires approximately 15 minutes when accomplished manually by cutting and sorting the chromosomes from a print (Ref. 1). Work is also in progress in automatic white blood cell classification (Ref. 2), in autoradiographic grain counting, and in numerous other areas.

Over the past three years, research in computer image enhancement at the Jet Propulsion Laboratory (JPL) has been experimentally applied to biomedical pictures in general and, particularly, to medical radiographs (Ref 3). The initial objective was simply to see if the computing techniques developed for processing spacecraft television pictures (Ref. 4) could be usefully extended to biomedical imagery. Rather than immediately attempting to apply the computer to a specific clinical or research problem, we have taken the more general approach of developing processing techniques applicable to classes of pictures such as pictures with high noise levels, pictures of low contrast, pictures having poor resolution, etc.

The main purpose of this paper is to describe some of the enhancement methods that have developed. As outlined in the next section, the frequency-domain approach to image system analysis was chosen as the most suitable means to relate the computer methods to the physical imaging system[1] and to the subject. Particular attention is paid to the interpretation of the system transfer function relative to the subject content. Following this, the most important computer enhancement technique, *digital filtering*, is discussed and illustrated with numerical examples. Details of filter evaluation and synthesis are covered in the appendix. The effects of various enhancement techniques, including linear and nonlinear filtering, are illustrated with examples of biomedical pictures before and after computer processing. An example of quantitative pictorial data analysis which uses the preceding enhancement techniques is also described.

II. Frequency Response Methods Applied to Imaging Systems

The general objective of picture enhancement is to make selected features easier to see. This might require suppression of useless data such as random noise and background shading or perhaps amplification of fine detail. Background shading becomes a problem when it is superimposed onto low contrast features. Usually, the subject itself is the source of the problem. For example, the small bones in the ear cannot generally be seen in a standard x-ray film because they absorb too little radiation relative to the larger surrounding bone mass. Random noise in an x-ray film results from the spatial fluctuations of the illuminating radiation. Similarly, film scanning systems inject noise into the image because of fluctuations in the light source and because of electrical noise in the output of the light-sensing device. Fine detail is lost by diffraction effects in optical systems or by fluorescent intensifying screens in x-ray systems. Clearly the imaging system as well as the subject must be taken into account when selecting a computer enhancement procedure, and to accomplish this a common method for describing each part of the system must be used. In many cases, frequency response techniques based on the Fourier transform can provide a common basis for relating the computer methods to the subject and to the imaging system.

With this technique, the subject or, more accurately, the signal composed of the spatial distribution of photons that results from illuminating the subject, is described by its Fourier or frequency-domain transform. That is, it is well known that any absolutely integrable signal can be decomposed into pure sinusoids of varying frequency, amplitude, and phase, and that the two representations, spatial and frequency, are precisely equivalent in the sense that each can theoretically be obtained from the other. For a picture system, frequency is measured as cycles per millimeter across the image.

Using frequency response methods, the imaging system is described by its *optical transfer function* (OTF) – also called more simply the *transfer function* – which is defined as the relative amplitude and phase response of the system to sinusoidal inputs of varying frequency. The amplitude response is commonly called the *modulation transfer function* (MTF). For an imaging system in which phase shift is absent, the OTF and the MTF are the same. If the imaging system is linear, which in this case means that the system output contains exactly the same frequencies as the input, then the signal spectrum of the output is equal to the product of the system transfer function and the input signal spectrum.[2]

[1] In this report the term imaging system means all parts of the system between the subject and the image digitizer.

[2] Certain parts of the system, such as the film, are not linear; but a linearizing correction can often be made when the image is processed with the computer. For film, the correction can be made if the optical density vs relative log exposure curve is known.

Under suitable conditions[3] the image digitizing process and many of the computer enhancement operations can be considered as linear extensions of the imaging system, and transfer functions for these parts can be derived. This in turn means that the entire system, from subject to computer enhancement, can be related by frequency response methods.

Before discussing the actual computer enhancement operations, it is useful to consider the effects of the imaging system on typical subjects in terms of the system frequency response.

For example, suppose two imaging systems A and B, with MTF as shown in Fig. 1, are to be compared. Since B produces equal or less attenuation than A at all frequencies, B will clearly reproduce the input scene more accurately. In particular, B will reproduce fine detail better than A since small features with sharp edges will usually result in an input signal whose spectrum has a greater proportion of its energy at high frequencies than does the signal resulting from large smooth features. It does not follow, however, that B would always be selected as the better system. For example, if a low-contrast shadow in an x-ray film were being sought and background noise was high, a system like A, that tends to reject high frequencies, might produce a more suitable film.

[3]The image must be sampled at a rate at least twice the highest frequency present in the signal. When a set of such measurements is taken, the sampled signal spectrum is a periodic version of the continuous signal spectrum, and under most circumstances the periodic components can safely be ignored.

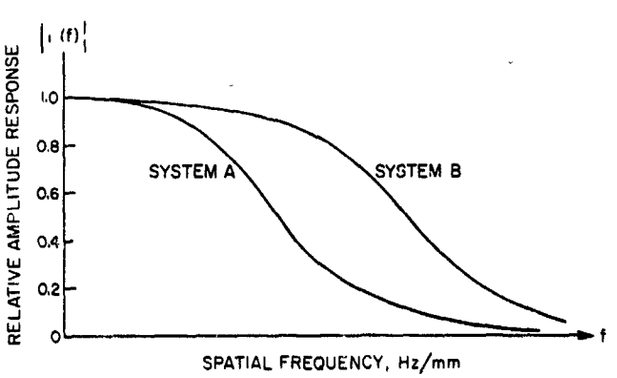

Fig. 1. Typical modulation transfer functions for two imaging systems

The behavior of the MTF at low frequencies is sometimes as important as it is at high frequencies. To illustrate this, consider the problem of locating a suspected hairline fracture in an x-ray film as shown in the drawing of a bone in Fig. 2(a). A plot of film density across the bone on the line shown might appear as in Fig. 2(b). The fracture appears as a low-amplitude, narrow (i.e., high-frequency) density change superimposed on the large, slowly changing, low-frequency signal representing the bone shadow. As shown, the fracture shadow probably would not be visible on the film. This example

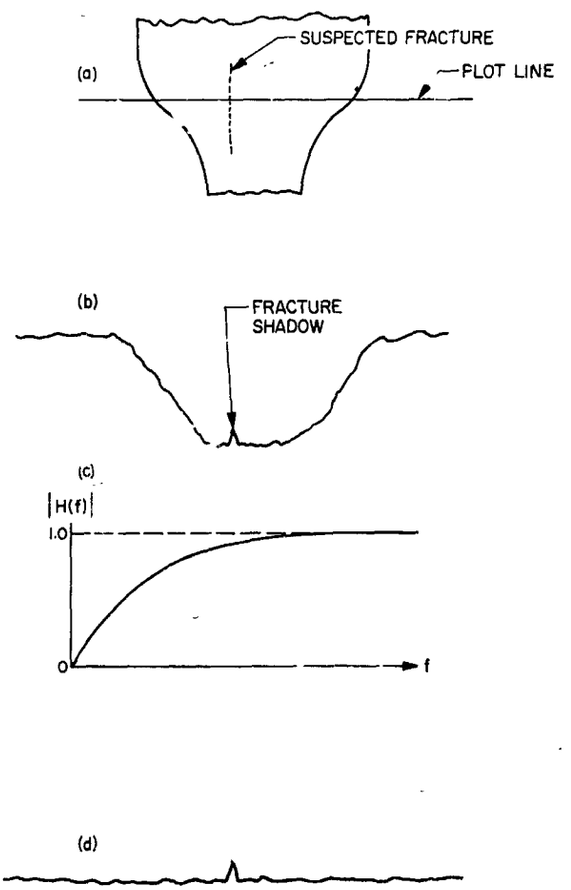

Fig. 2. Illustration of the processing steps for removing background shading to enhance small low-contrast feature: (a) representation of an X-ray image of a bone containing a suspected hairline fracture shown as a dotted line; (b) typical density plot that might be observed along a single line across the film; (c) modulation transfer function of a filter that could be used to remove the background; (d) density plot after filtering, showing background removal

demonstrates that sometimes it is desirable to reproduce high frequencies but *not* low frequencies. If a system were selected that has an MTF as shown in Fig. 2(c), the low frequencies would be rejected and the plot line through the film would look as shown by Fig. 2(d). At this point, an increase in contrast would bring out the fracture shadow.

As another example, consider the pictures generated by isotope scanners which frequently contain narrow bars of unexposed film between each recorded scan line. If the unwanted bars were spaced every T_1 millimeters down the image, an imaging system that would reject the bars would require a two-dimensional MTF like that shown in Fig. 3. Designing an actual system with such a transfer function would be quite difficult if not impossible, but a digital filter with zero gain near frequency $f_1 = 1/T_1$ and near-unity gain at all other frequencies of interest could easily be obtained. When a digital filter is applied to a picture, a new system MTF can be determined that includes the effect of the filter. In the linear case, this new MTF is basically the product of the original imaging system MTF and the filter MTF. Thus application of the digital filter first described to a picture from an isotope scanner with a normal MTF would produce an effective overall system MTF like that shown in Fig. 3.

Many, although not all, computer image enhancement techniques are linear operations so that once a transfer function for a particular computer operation is determined, a new system MTF can be determined which includes the physical parts of the imaging system, the film digitizer, and the computer operations.

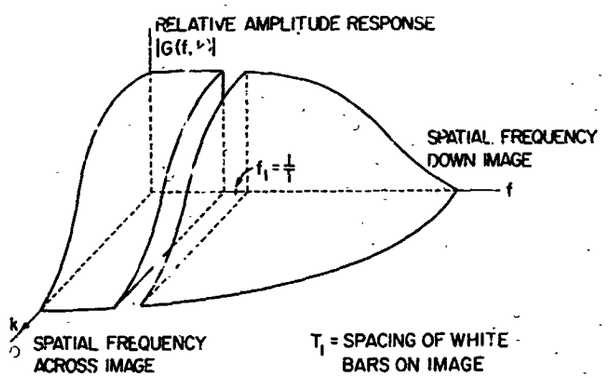

Fig. 3. Modulation transfer function designed to reject horizontal bars which are typical of films generated by isotope scanners. Bars are assumed to appear every T_1 millimeters

III. Digital Filters

One of the most important linear image enhancement techniques is that of *filtering*. The operation of digital filters can most conveniently be explained in the spatial domain while classification of the different types of filters is more easily accomplished using a frequency domain description. Methods for calculating the MTF of a given filter and for obtaining a filter with a specified MTF are described in the appendix.

A. Definition of a Digital Filter

An electronic filter produces an output voltage that depends on weighting of the past signals. A digital filter operates in the same manner except that both past and future signals are available and, of course, the signals are discrete.

Let $(x_0, x_1, \cdots, x_n)$ be a sequence of numbers derived by sampling and digitizing a continuous signal such as the optical density along a line on a film, and assume samples are taken every T millimeters along the line. Consider a simple three-point filter that replaces the point x_n with the average of the points x_{n-1}, x_n, x_{n+1}. If y_n is the filtered point at position n, then

$$y_n = 1/3\, x_{n-1} + 1/3\, x_n + 1/3\, x_{n+1}$$

Similarly, the next filtered point y_{n+1} is obtained as

$$y_{n+1} = 1/3\, x_n + 1/3\, x_{n+1} + 1/3\, x_{n+2}$$

The values 1/3 are the filter weights, which in general are not necessarily equal. The main filtering relation, using $2K + 1$ weights

$$g = (g_{-K}, \cdots, g_{-1}, g_0, g_1, \cdots, g_K)$$

is

$$y_n = \sum_{k=-K}^{K} g_k\, x_{n-k} \qquad (1)$$

Thus, filtering is obtained by a weighted moving average.

Equation (1), the filter equation, is readily extended to two dimensions. Let the unfiltered signal be represented by an array of numbers ($x_{m,n}$, $m = 0.1, \cdots, M$, $n = 0,1, \cdots, N$) and the filter weights by the array

$$g = (g_{k,l}, k = 0, \pm 1, \pm K; l = 0, \pm 1, \cdots, \pm L)$$

Then if $y_{m,n}$ is a filtered point, the two-dimensional filter equation becomes

$$y_{m,n} = \sum_{k=-K}^{K} \sum_{l=-L}^{L} g_{k,l}\, x_{m-k,\, n-l}$$

A two-dimensional averaging filter analogous to the three-point one-dimensional averaging filter just discussed is one that averages the nearest nine points including the nearest three points on each line above and below the center point $x_{m,n}$ as well as $x_{m,n}$ and the points

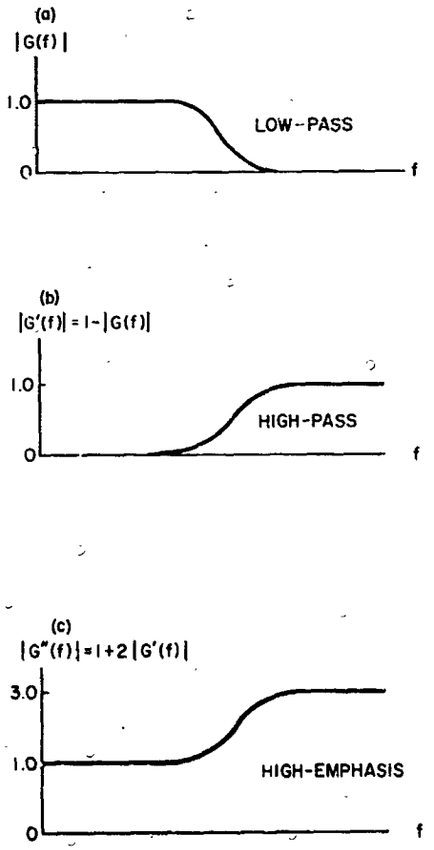

Fig. 4. Typical filter transfer functions: (a) low-pass; (b) high-pass; (c) high-frequency restoration. Filters (b) and (c) derived from filter (a)

on either side of the same line. Most of the ideas that follow are easily extended from one to two dimensions so that, in the interest of keeping the notation simpler, only the one-dimensional filter will be presented in most cases.

B. Filter Classes

The three-point equal-weight filter previously discussed is an example of a *low-pass filter* whose purpose, as the name implies, is to pass low-frequency signal components and reject the high ones. A typical modulation transfer function of a low-pass filter is shown in Fig. 4(a).

A *high-pass filter* has the opposite function of removing low-frequency signals and passing the high-frequency signals. One obvious way to achieve such a filter is to subtract, point-by-point, a low-passed picture from the original. Rather than actually perform such a two-step operation, it is possible to derive weights that directly high-pass the picture. Suppose x_n is the unfiltered input, y_n the output from a low-pass filter and y'_n the output from a high-pass filter. Let $g = (g_{-k}, \cdots, g_k)$ be the low-pass weights and $g' = (g'_{-k}, \cdots, g'_k)$ be the high-pass weights. If the low-pass picture is subtracted from the unfiltered picture, point-by-point,

$$y'_n = x_n - y_n$$

and then expressions for y'_n and y_n according to the filter Eq. (1) are substituted above

$$\sum_{k=-K}^{K} g'_k\, x_{n-k} = x_n - \sum_{k=-K}^{K} g_k\, x_{n-k}$$

Equating coefficients of x_{n-k} on either side of the equality, it follows that

$$g'_k = \delta(k) - g_k$$

where

$$\delta(k) = 1 \text{ for } k = 0$$
$$= 0 \text{ otherwise.}$$

As shown in the appendix, if the low-pass filter has MTF $G(f)$ as shown in Fig. 4(a), then the high-pass filter just derived has MTF $G'(f) = 1 - G(f)$. A plot of $|G(f)|$ is shown in Fig. 4(b).

Consider another type of filter that might be called a *high-emphasis* or high-frequency restoration filter. This

filter passes low-frequency signals unchanged and amplifies high-frequency signals. Pre-emphasis networks in hi-fi systems are filters of this type. Applied to a picture, this type of filter sharpens edges and generally magnifies small detail. A high-pass filter and a high-emphasis filter are similar except the high-pass filter removes the low frequencies while the high-emphasis does not. In fact, a high-emphasis filter can be derived from a high-pass filter by multiplying all the high-pass weights g'_k by a constant and then adding one to the center weight. That is, if g''_k is a high-emphasis filter weight, and A is a constant,

$$g''_k = \delta(k) + Ag'_k$$

Multiplication of every weight by a constant is equivalent to multiplying every value of the MTF by the same constant. It also can be interpreted as stretching the contrast of the picture by this constant. Also, adding one to the central weight adds one to the MTF at every point. Thus, for A = 2, the high-emphasis filter derived from the high-pass filter of Fig. 4(b) would appear as shown in Fig. 4(c).

Instead of smoothing by simple averaging, higher degrees of polynomial smoothing may be applied. For example, suppose a smoothed point is obtained by evaluating a third-degree least-squares polynomial fit to the nearest five points. It can be shown that such an operation is equivalent to applying the filtering equation, Eq. (1), using the following weights:

$$g = (-3/35, 12/35, 17/35, 12/35, -3/35)$$

To determine how this filter differs in its effect on the signal from the equal-weight filter or from any other filter, the modulation transfer function can be computed.

As described in the appendix, the transfer function $G(f)$ of a filter represented by weights $g = (g_{-k}, \cdots, g_0, \cdots, g_k)$ is obtained as the Fourier transform of the weights. The three-point equal-weight filter, for example, defined by

$$g = (1/3, 1/3, 1/3)$$

has a transfer function obtained as

$$G(f) = 1/3 + 1/3 \cos 2\pi f$$

where a sampling period of one is assumed, so f represents cycles per sample.

A plot of $|G(f)|$ is shown in Fig. 5(a). The dotted lines indicate negative values of $G(f)$ which represents a 180 deg phase shift. That is, if the input to the filter is a sine wave whose frequency is in this range, the output would be the negative of the input. Figure 5(b) shows the MTF for the five-point equal-weight filter. As would be anticipated, five-point averaging results in greater

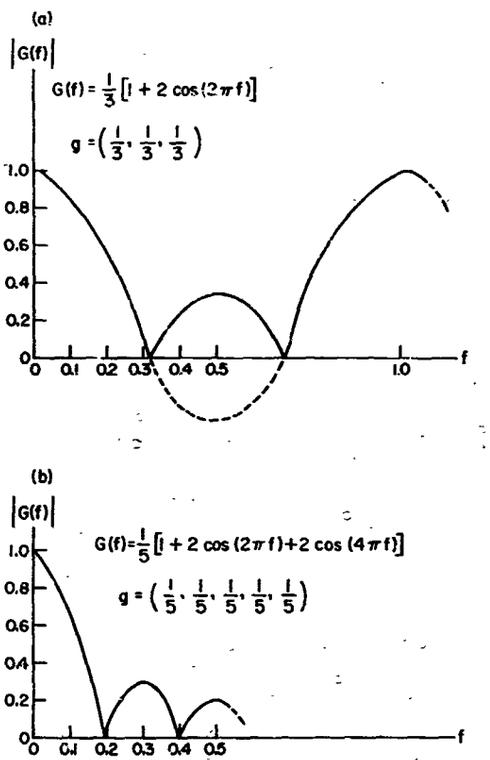

Fig. 5. Transfer functions for equal-weight filters: (a) three-point; (b) five-point

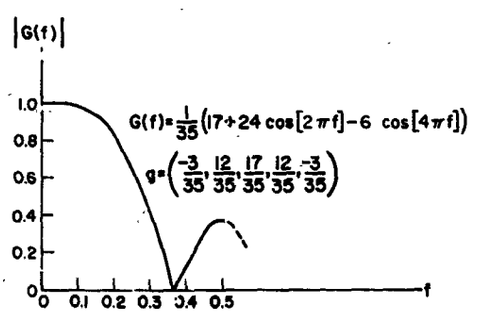

Fig. 6. Transfer function for five-point third-degree least-squares filter

attenuation of high frequencies than three-point averaging. In comparison, the MTF of the five-point third-degree filter shown in Fig. 6 produces less attenuation than either equal-weight filter.

For all of the filters discussed above, the weights were selected first and then the effective filter MTF was calculated. To obtain a filter with a given MTF, the weights are calculated by taking the inverse Fourier transform of the specified MTF (see appendix).

IV. Computer Image Enhancement Applications

The before-and-after examples of computer-enhanced pictures described in this section illustrate (1) four classes of two-dimensional linear filter, (2) nonlinear filters, including nonlinear contrast enhancers, and (3) image subtraction. The types of images processed include x-ray films, isotope scanner films, and photomicrographs.

All of the pictures were scanned with a cathode-ray tube flying spot scanner and digitized to six *bits* (0–63 counts). Although the system provides a maximum of 1200 scan lines per inch, it accepts film only about 2 in. square so that larger film, such as x-ray film, must first be photographically reduced and then scanned. Considerable degradation results from this reduction process however, and, in addition, some random noise is injected into the image by the film scanner. Photographic reduction can be eliminated by directly scanning the original, full-size film with high-quality image dissector television systems or with mechanical scanners. Scanning noise can easily be minimized either by leaving the scanning spot on each picture point for a long period and then integrating the resulting signal from the photosensing device, or by scanning a picture several times at a normal rate and then averaging the frames in the computer. Although this latter technique has recently been adopted at JPL with very good results, most of the pictures shown in this section were obtained with a single fast scan that has left unnecessarily high noise levels. To demonstrate the effect of the computer processing independently from the scanning losses, the enhanced pictures that follow are compared with the unenhanced but digitized versions rather than with the original films.

A. Low-Pass Filter Applications

The removal of high-frequency components from a picture may be desirable in a variety of situations. The most common application is made to pictures containing excessive random noise which makes large low-contrast features difficult to see clearly. Low-pass filtering of noisy pictures is frequently necessary when the computer is used for pattern recognition or measurement purposes. Occasions also arise in which it is useful to remove non-random high-frequency structure—such as sharp edges—that are not important and make the rest of the picture difficult to view.

As an example of the application of a low-pass filter to a picture, consider the tomograph section of the ear shown in Fig. 7. This picture is composed of 1000 lines and 1000 elements a line. The sample and line spacing on the original film were 25 microns. The feature to be enhanced is the cochlea, the light spiral in the upper half

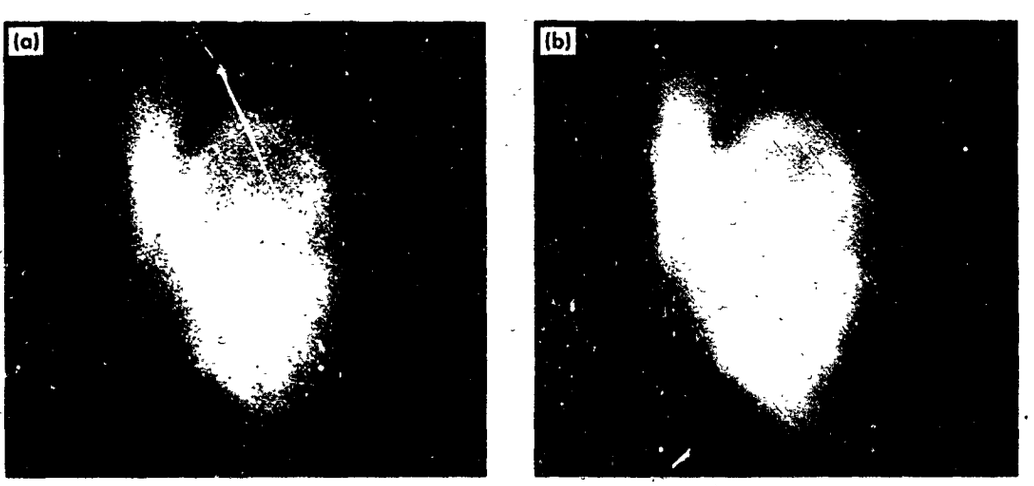

Fig. 7. X-ray tomograph of cochlea (*light spiral*): (a) unprocessed; (b) after 31 × 31 equal-weight low-pass filter

of the picture. In this case, the noise-like structure results from the spatial fluctuations of the exposing radiation which is characteristic of tomographic imaging systems. An averaging filter was selected that consisted of equal weights in a 31 × 31 array. The size was chosen large enough to remove the noise but not so large as to remove the image of the cochlea which varied in size from about 30 to 50 samples across.

A second example of the use of a low-pass filter is shown in Fig. 8 in which an unprocessed picture of the calcaneus on the left and a filtered version on the right was obtained by applying a 7 × 7 equal-weight filter. In this particular picture, the viewer does not have great difficulty following the trabecular shadows (the vertical light streaks); but when the computer was later required to detect and measure the width of each shadow, the job was made extremely difficult by the high-frequency noise. An example of a picture in which disturbing nonrandom structure appears that can be removed by filtering is shown in Fig. 9(a). This chest film generated by an isotope scanner has characteristic square-like picture elements and white bars between each line that obscure useful information by attracting the eye. The lines were first removed by a computer process to be described later, as shown in Fig. 9(b); then, an 11 × 11 equal-weight low-pass filter was applied to eliminate the square-like structure of the original individual picture elements, as shown in Fig. 9(c).

Radiograph noise resulting from quantum fluctuations in the source is not concentrated at the high-frequency end of the spectrum as might be assumed from the salt-and-pepper effect. Rather, the noise is somewhat evenly distributed over all frequencies passed by the system. Consequently, a simple low-pass filter cannot remove noise in many cases and may even cause a poorer picture than the original by producing a clumping or mottled effect such as that shown in the radiograph of the spine in Fig. 10. This effect is less noticeable in Figs. 7 and 8 because considerably more of the high-frequency signal was removed from these pictures.

B. High-Pass Filter Applications

A common problem in x-ray photography is the visualization of small low-contrast features when they are superimposed onto a very dark or very light background. Direct contrast enhancement will not improve the image because the film or the print will saturate at maximum white or black. The solution is to apply a high-pass filter that removes the background by converting constant or very slowly changing dark or light areas to grey. The smaller low-contrast superimposed feature also moves to grey but now contrast enhancement may be applied without saturation occurring.

The basic shape of a high-pass filter is shown in Fig. 4(b). Removing the constant or dc component of an electrical signal generally means centering the signal about zero. For the type of picture system discussed here, in which maximum white is represented by zero and maximum black by 63, the removal of the dc component means centering the picture about mid-grey, represented by 31. Thus the filtering equation Eq. (1) becomes

$$y_n = 31 + \sum_{k=-K}^{K} g_k x_n$$

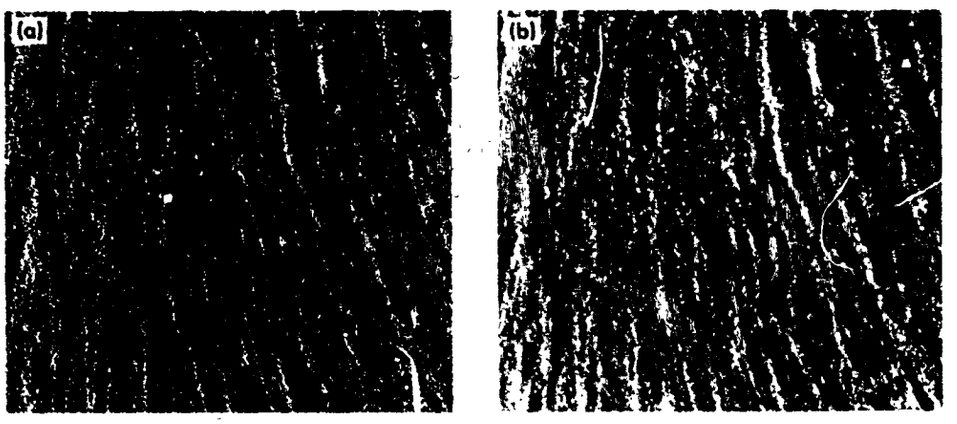

Fig. 8. Radiograph of calcaneus: (a) unprocessed; (b) after 7 × 7 equal-weight low-pass filter

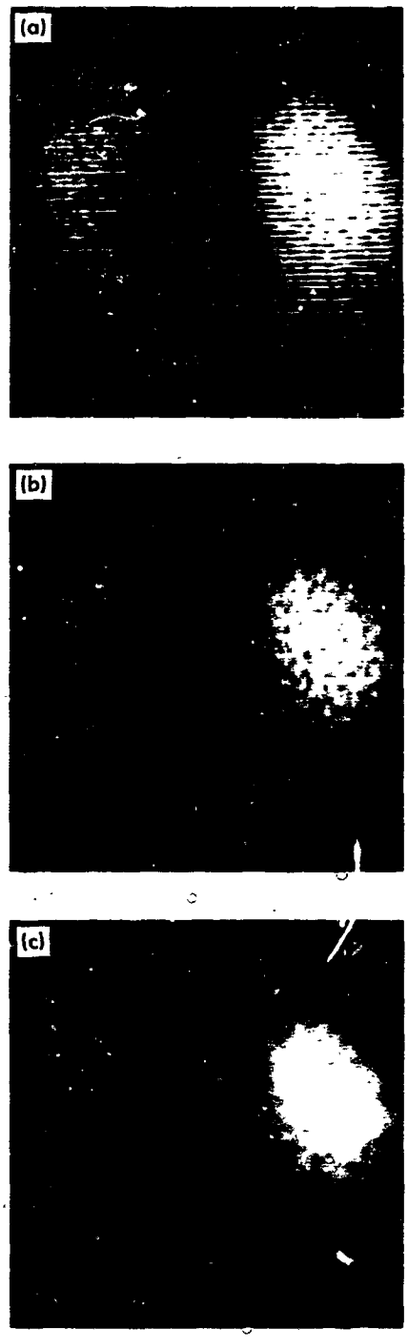

Fig. 9. Radioisotope scanner chest film: (a) unprocessed image; (b) after removal of scan lines; (c) after 11 × 11 equal-weight low-pass filter applied to (b)

An example of before-and-after high-pass filtering is shown in Fig. 11. The left figure, a radiograph of a bone, shows that an opaque dye has been injected into the blood. When the viewing illumination was varied on the original film, the blood vessels alongside the bone and those in line with the bone could be seen. Similarly, a darker print would bring out those alongside the bone, while probably rendering the bone itself solid black. The problem is simply that the range of film density is too large. The high-pass filter narrows that range by removing background which forces the data to more satisfactorily match the film characteristics. The information that is thrown away – the background shading – is irrelevant. Figure 11 shows the result of first applying a high-pass filter and then increasing contrast by a factor of four. Since increasing contrast by four is equivalent to applying a filter that uniformly amplifies all signal frequencies by four, a substantial amount of noise amplification takes place as is clear in this example.

A high-pass filter applied to the ear tomograph of Fig. 7 is shown in Fig. 12 on the left. The result of increasing the contrast is shown on the right.

The filter weights for this example are defined as

$$g_{k,l} = 1 - \frac{1}{(2K+1)(2L+1)} \quad \text{for } k = 0, l = 0$$

$$= -\frac{1}{(2K+1)(2L+1)} \quad \text{otherwise.}$$

Application of these weights using Eq. (1) is equivalent to subtracting the average of the $(2K + 1) \cdot (2L + 1)$ points surrounding x_n from x_n itself. Then, as previously indicated, this difference is added to 31 to produce the filtered point y_n. With this interpretation in mind, it becomes clear that the size of the filter-weight matrix must be substantially larger than the largest feature to be left in the picture so that the feature will not contribute too heavily to the local average and possibly be subtracted from the picture. For the ear tomograph a filter size of 55 × 55 was selected. Since the high-pass filter was applied to a picture that had previously been low-passed, the overall effect is that of a band-pass filter that removes both high and low frequencies. This same result could as easily be obtained from a single band-pass filter applied to the unprocessed picture.

A last example of high-pass filtering is shown in Fig. 13 which shows pictures of the calcaneus before and after filtering. In this case, the filtering was not done to enhance but to prepare the picture signal for a computer quantitation program. The shading shown in Fig. 13 (*left*)

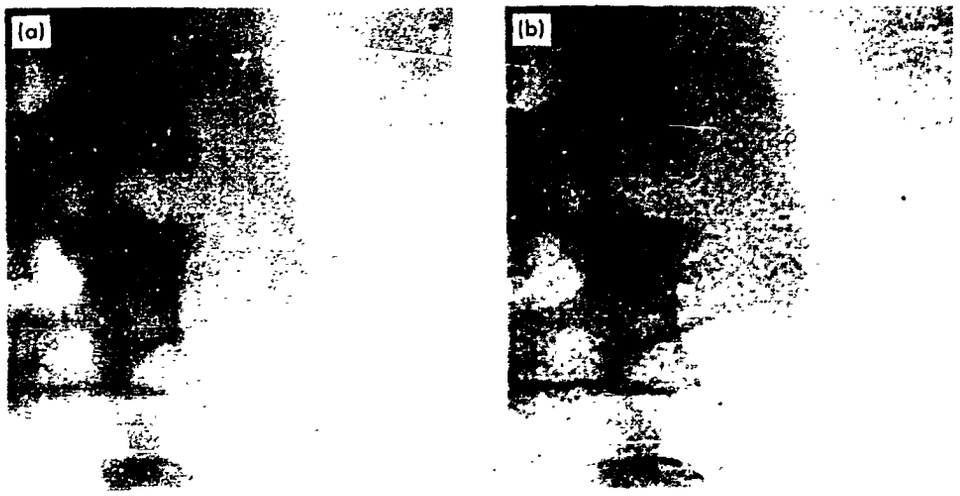

Fig. 10. Radiograph of spine showing mottling caused by removing only high-frequency signal components when random noise is present at all frequencies: (a) unprocessed; (b) after low-pass filter

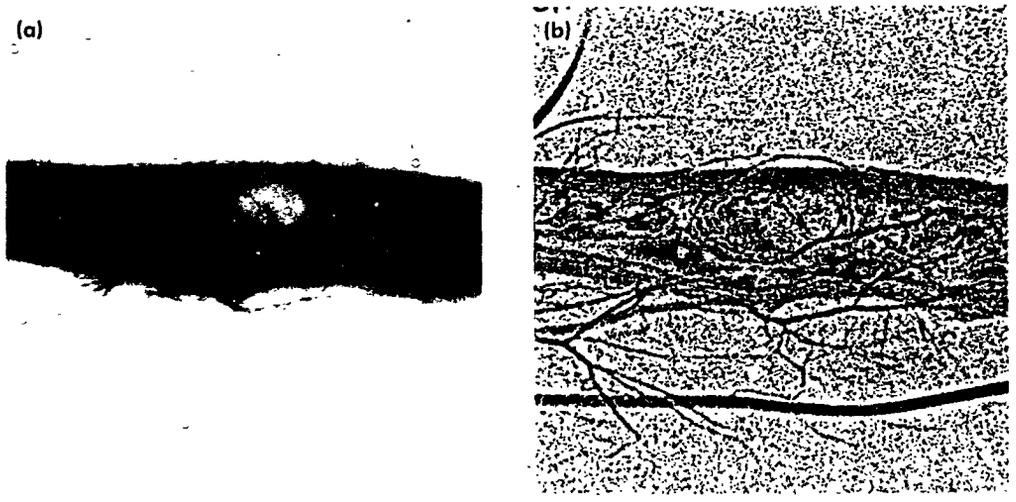

Fig. 11. Angiogram of bone showing background removal: (a) unprocessed; (b) after high-pass filter and contrast enhancement by factor of four

was removed with a one-dimensional filter that subtracted from each point the average of the nearest 101 points. Since the shading did not change abruptly from line to line, a one-dimensional filter was assumed sufficient. Although the shading is removed, some of the horizontal trabecular structure is also removed,[1] an effect that was avoided in later applications by using a two-dimensional filter.

[1]This effect could not actually be seen, but was detected by subsequent computer measurement of the horizontal shadow widths.

C. High-Frequency Restoration Filters

Consider an imaging system with a modulation transfer function $H(f)$, indicated by Fig. 14(a), that shows the usual dropoff in response at high frequencies. Restoration of this loss could be accomplished by a filter with an MTF, $G(f)$, equal to $1/H(f)$, as shown in Fig. 14(b). Thus the overall MTF of the system including the filter becomes

$$M(f) = H(f) \cdot G(f)$$

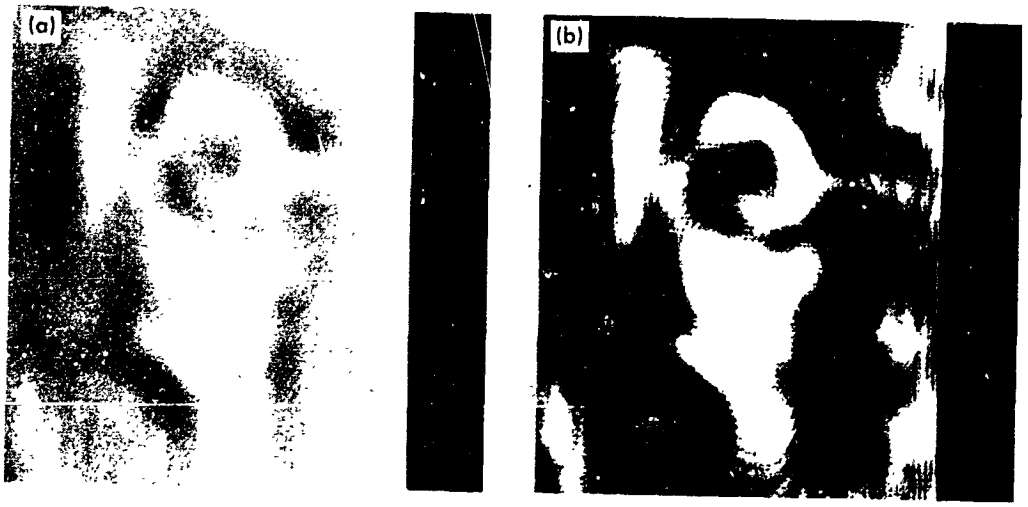

Fig. 12. Tomograph of the ear: (a) after high-pass filter; (b) after high-pass filter and contrast enhancement

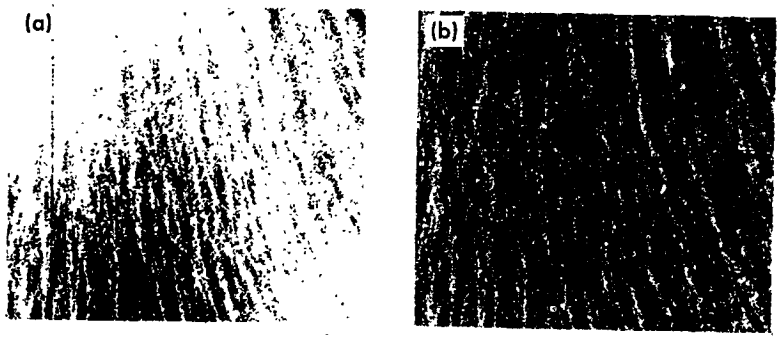

Fig. 13. Radiograph of calcaneus showing background removal: (a) unprocessed; (b) after 101-weight one-dimensional high-pass filter

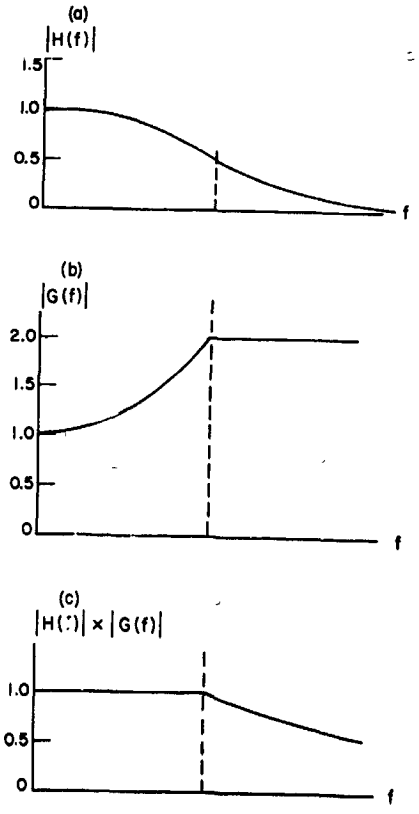

Fig. 14. Diagram showing effect of high-frequency restoration: (a) typical system MTF; (b) filter MTF designed as inverse of the system MTF; (c) MTF of overall system including filter

as shown in Fig. 14(c). Instead of continuing as the inverse of $H(f)$, the filter must level off at some point to avoid excessive amplification of system noise.

Considerable work has been devoted to measuring the MTF of imaging systems. For example, the MTF of fluorescent intensifying screen and film combinations used in x-ray systems has been obtained by Rossman (Refs. 5, 6) and Morgan (Ref. 7) as well as the MTF of the x-ray focal spot as a function of its size and geometry by Doi (Ref. 8). It does not follow, however, that if the x-ray system MTF were known, the optimum high-frequency restoration filter would be the one whose transfer function was the inverse of the system MTF. The reason for this, aside from the problem of noise amplification, is that a distorted system response is as likely to enhance *important* information as a flat system response. The high-pass filter examples demonstrated this. The important point is that optimization depends not only on the imaging system itself, but also on the subject, the (medical) purpose of the film, and the perceptual response of the viewer. These areas are currently under investigation by Rossman (Ref. 9), Tuddenham (Ref. 10) and others.

For systems with very high signal-to-noise ratio, high-frequency restoration filters are quite effective. Figures 15 and 16 show examples of this type of filtering

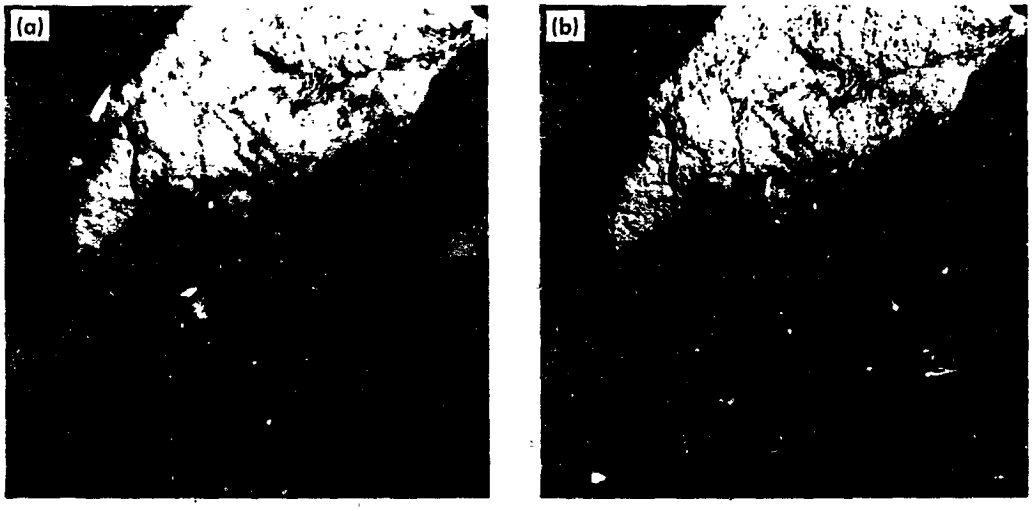

Fig. 15. *Surveyor I* picture of lunar surface: (a) unprocessed; (b) after high-frequency restoration filter

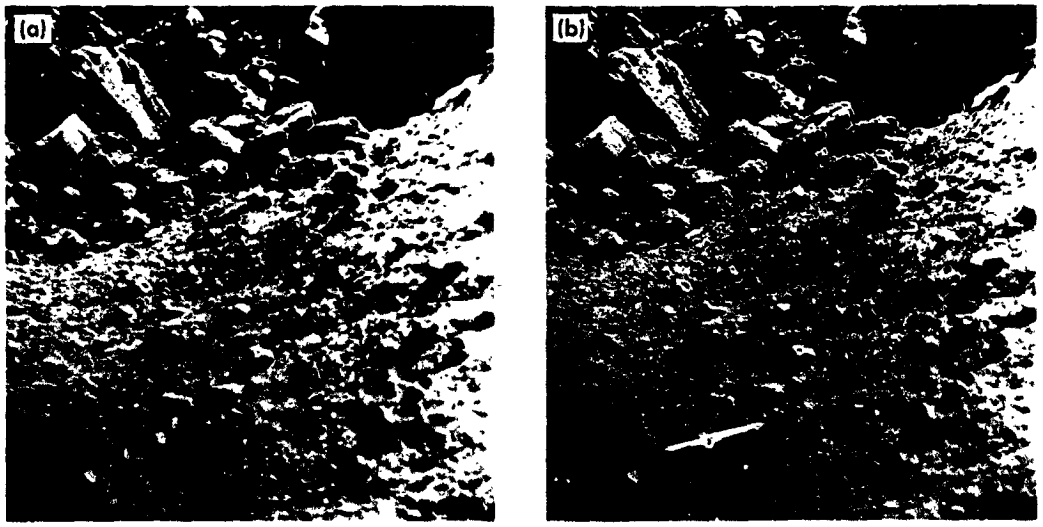

Fig. 16. *Surveyor VII* picture of lunar surface: (a) unprocessed; (b) after high-frequency restoration filter

applied to pictures of the lunar surface televised by the *Surveyor* spacecraft for which, it might be noted, the received video signals were directly sampled and digitized without intermediate film scanning.

Applying high-frequency restoration to photomicrographs also provides some degree of detail sharpening, as is seen in the chromosome pictures in Fig. 17.

Unfortunately, the noise level in x-ray films is so high that high-frequency restoration filtering is relatively ineffective. An example of this type of filter applied to a noisy x-ray picture is shown in Fig. 18. Some improvement in resolution of the intermediate-size blood vessels can be seen (*arrows*) but the very fine blood vessels are still lost in the noise. This does not mean that further improvement in resolution cannot be obtained, however.

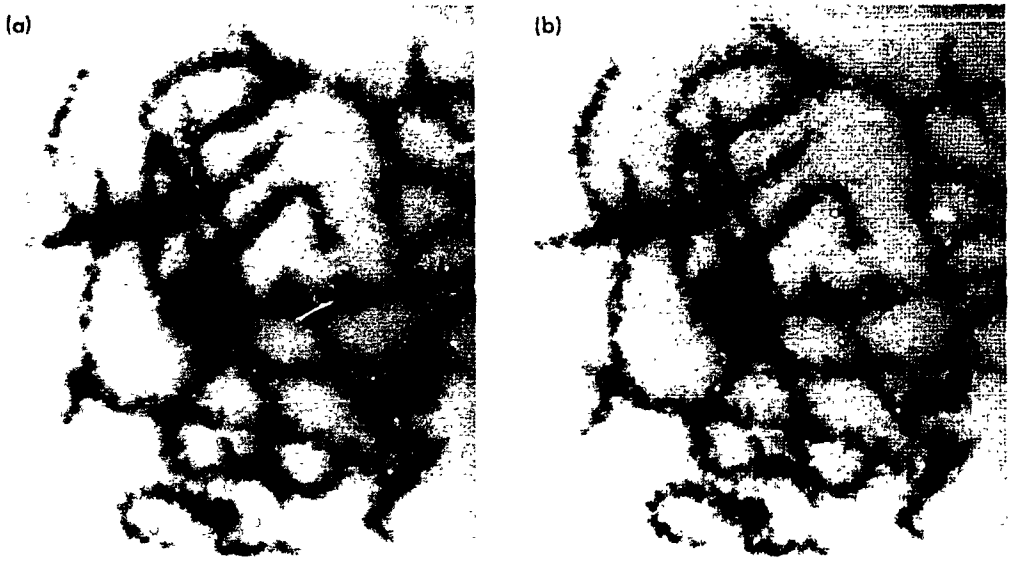

Fig. 17. Photomicrograph of human chromosomes: (a) unprocessed; (b) after high-frequency restoration filter

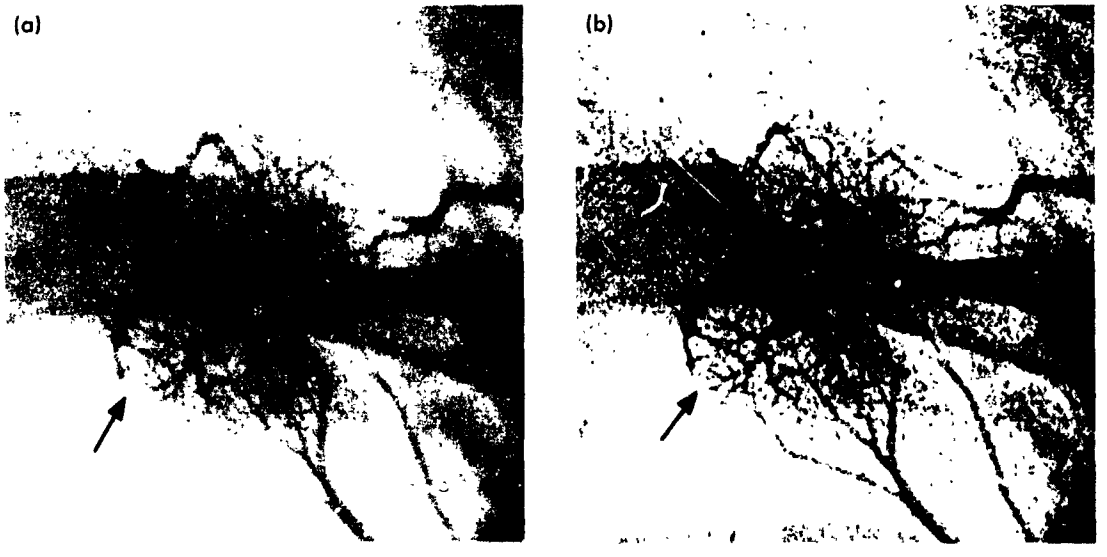

Fig. 18. Pulmonary angiogram showing effect of high-frequency restoration: (a) unprocessed; (b) after high-frequency restoration, small blood vessel sharpened by filtering (*arrow*)

It does mean that the filters must be tailored more to image content than to the imaging system. Filters of this type are described in the next section.

D. Feature-Selective Filters

Feature-selective filters operate by cross-correlating the picture with a matrix of weights that geometrically resembles the feature to be enhanced. If, for example, vertical lines are to be enhanced, the filter weights are made positive along a vertical line in the center of the matrix and negative otherwise so that the output of the filter is a maximum when the filter is centered on a vertical line in the picture. The weights shown in Fig. 19 were selected to enhance the blood vessel shadows in the angiogram shown in Fig. 20 (*upper*). The arrow points to some blood vessels faintly visible in the unprocessed film and better defined in the filtered version. The two lower pictures represent further enhancement by subtraction methods to be discussed later.

Filters of this type can either enhance or remove selected features. A radiograph of a thin section of bone from an excised vertebra is shown in Fig. 21 (a). A subsequent computing requirement to measure, first, the

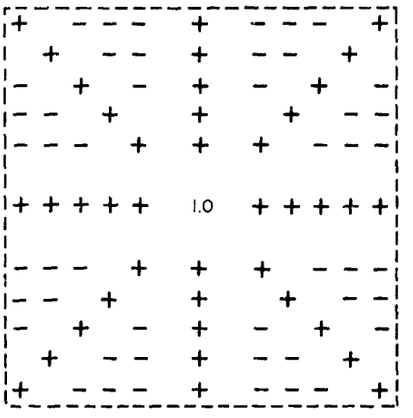

Fig. 19. Feature-selective filter used to enhance lines that are linear or nearly linear over short distance

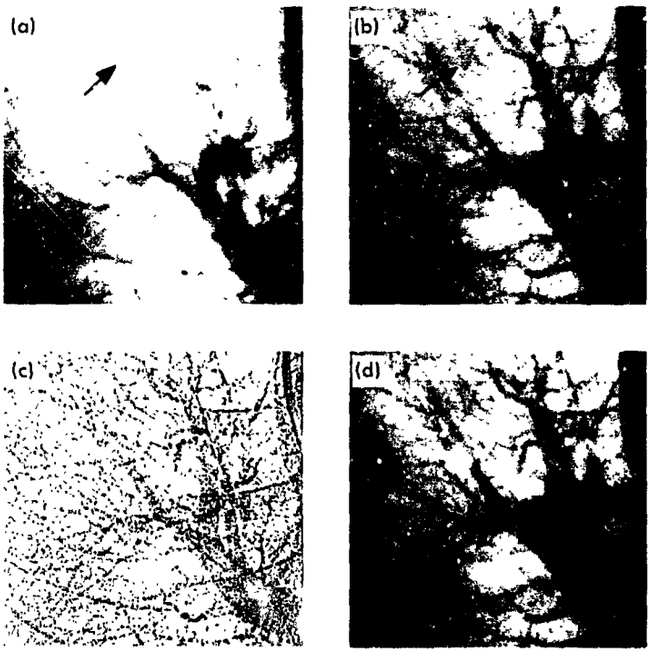

Fig. 20. Pulmonary angiogram showing result of applying filter designed to enhance straight lines: (a) unprocessed picture; (b) after application of filter shown in Fig. 19. Blood vessels faintly visible on the unprocessed picture but more clearly defined on filtered picture *(arrow)*; (c) result of subtracting unprocessed picture from filtered picture to emphasize changes caused by filtering; only positive differences retained, and contrast greatly increased; (d) result of adding four times the positive-difference picture to unprocessed picture

width of the vertical trabecular shadows and, then, the width of the horizontal shadows made it desirable to remove those shadows not being measured in each case. The upper right image in Fig. 21 shows the vertebra with the non-vertical shadows removed, and the bottom picture shows the result of removing most of the non-horizontal trabecular shadows.

E. Nonlinear Filtering and Contrast Enhancement

Nonlinearity in digital filters occurs when the filter output, as defined by Eq. (1), is truncated, either deliberately to produce a specialized effect, or unavoidably when the output exceeds the allowable grey-scale range (i.e., saturation). The filtering procedure used to remove the white lines from the isotope scanner image of Fig. 9 is an example of intentional nonlinearity. Filtering was accomplished in two steps. First, Eq. (1) was applied with the following vertical weights:

$$g = (1/6,\ 1/6,\ 1/6,\ 0,\ 0,\ 0,\ 1/6,\ 1/6,\ 1/6).$$

Next, the filtered point y_n was compared with the corresponding input x_n. If the filtered point was larger than the input, as would likely be so if the input point was part of a line to be removed (white is represented by a low number), the filtered point was accepted as is. Otherwise, the input point was substituted. The effect of this procedure was to leave the picture unchanged whenever the filter was not centered on a line.

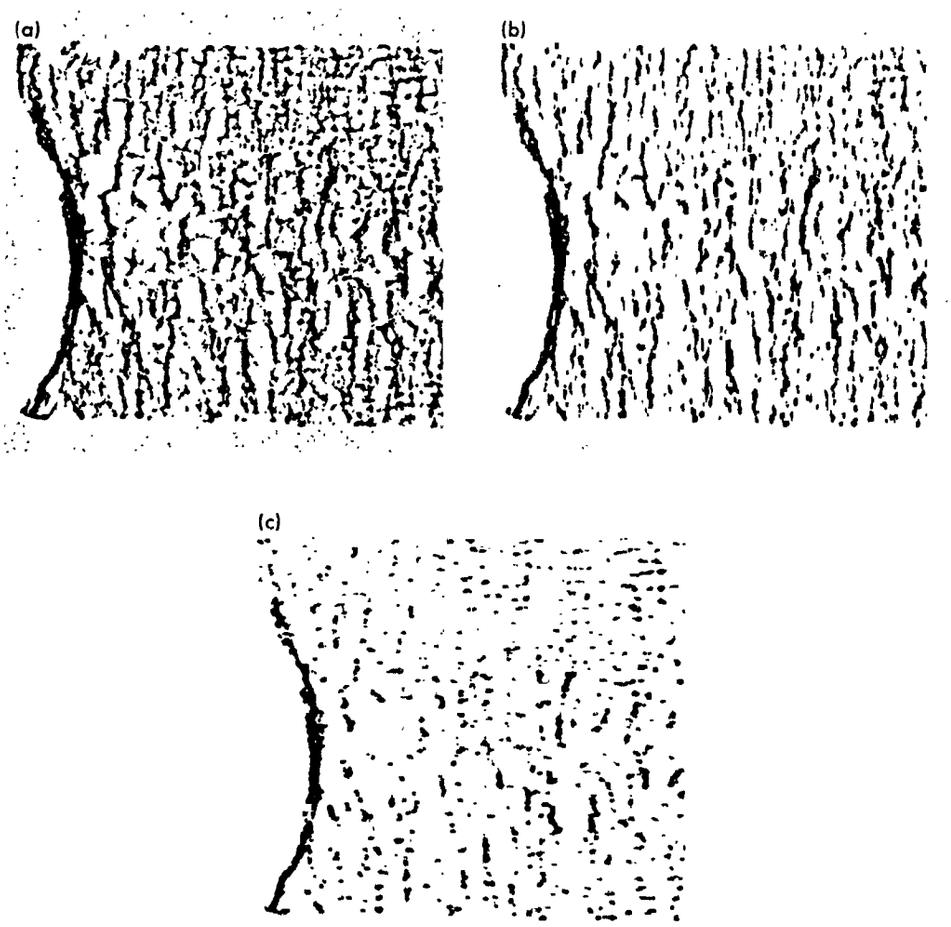

Fig. 21. Radiograph of thin section of vertebra showing effect of filters designed to remove non-vertical and non-horizontal trabecular shadows: (a) unprocessed picture; (b) after filter to remove non-vertical shadows; (c) after filter to remove non-horizontal shadows

Simple contrast enhancement of the type shown in Fig. 22(a) in which input points having values between A and B are linearly stretched to full scale, is an example of filter nonlinearity resulting from saturation. A more interesting procedure is to divide the input into several intervals and stretch each interval simultaneously. As shown in Fig. 22(b), the input range is divided into four intervals and each expanded to full scale. The effect of such a procedure on a picture is to display everything in the picture at a high contrast. An example four- and eight-cycle expansion applied to a photograph of the retina is shown in Fig. 23 (*lower*). In particular, note the improved definition of blood vessel wall. The original picture (*upper left*) and an enlarged version of the area of interest (*upper right*) are shown. There is, of course, a substantial amount of artifact created by this procedure, so caution must be exercised in the interpretation of these pictures.

F. Image Subtraction

Subtraction of radiographic images is a useful method for amplifying differences between two pictures. In particular, for an angiographic series, subtraction of the pre-dye picture from pictures which include the dye is an effective means for removing bone shadows from the picture in order to see the fine blood vessel structure more clearly. Optical subtraction methods are in clinical

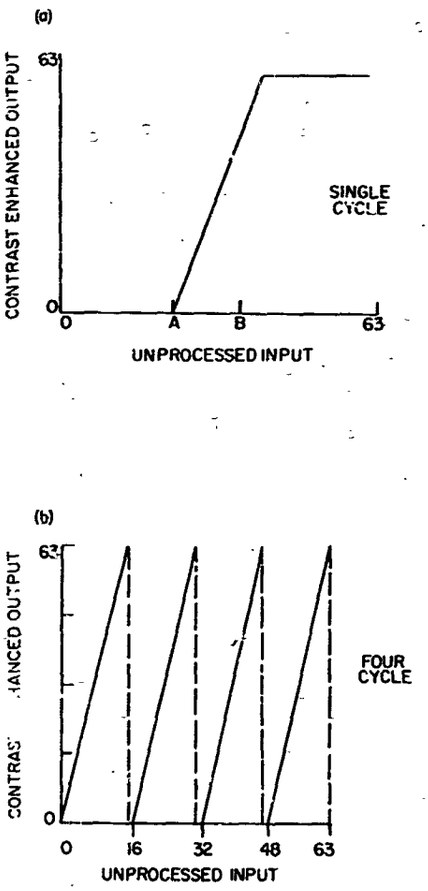

Fig. 22. Transfer characteristic relating picture input and output for contrast enhancement: (a) simple enhancement; (b) four-cycle enhancement

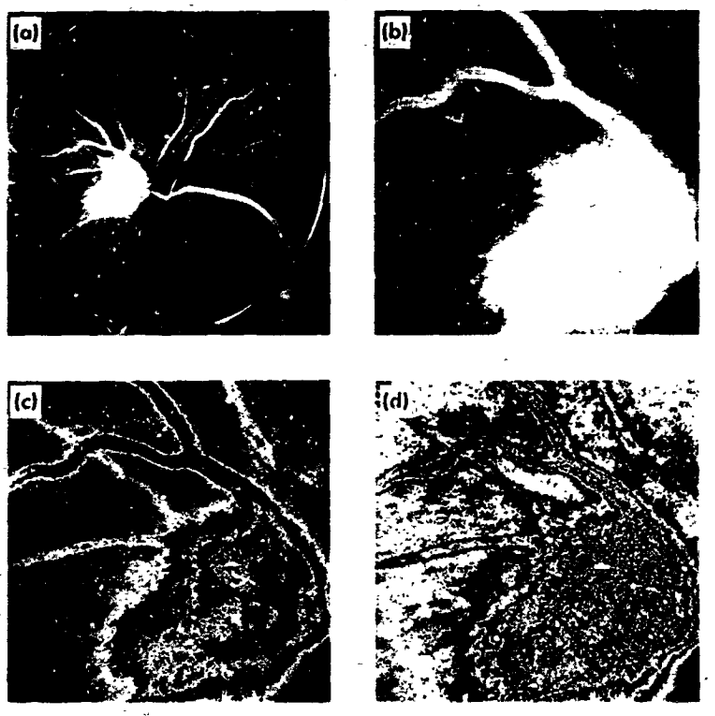

Fig. 23. Retina photograph showing multiple-cycle contrast enhancement: (a) unprocessed picture; (b) enlargement of section to be enhanced; (c) result of four-cycle overlapping contrast enhancement as indicated in Fig. 22(b); (d) result of eight-cycle overlapping contrast enhancement

use today for rigid structures such as the skull (Ref. 11). For nonrigid structures such as the chest, optical subtraction can still be performed, but difficulties in matching large areas usually restrict the subtraction to a small area.

Image subtraction can also be performed by computer and, with mismatched pictures such as just described, the computer can be used to geometrically distort one picture to match the second. An example of such an operation on a pair of chest films is described in Ref. 3. An advantage of computer subtraction over optical subtraction is that the difference picture is immediately available for further enhancement such as high-frequency restoration. Also, with cross-correlation techniques the *best match* between pictures could be automatically accomplished by the computer and would probably be superior to a match obtained by manually superimposing one film on another.

Subtraction of an unprocessed picture from a filtered picture can also be a useful way to evaluate the filter itself when changes produced by the filter are rather subtle. The result of subtracting two pictures in this manner is shown in Fig. 20(c). Figure 20(d) was obtained by multiplying the positive part of the difference picture by four and adding this difference to the unprocessed picture.

V. The Use of Computers To Make Quantitative Measurements on X-ray Film

A recent application that promises to be of great value is the use of a computer to make numerical measurements on x-ray film. In one of the earliest applications, by Becker et al. (Ref. 12), a computer and flying-spot scanner were used to measure the maximum transverse diameter of the heart shadow and the maximum transverse diameter of the rib cage shadow. Their method summed each column of a digitized x-ray film of the chest and then used the sums, plotted as a function of distance across the chest, to detect the location of the required features.

A large amount of current research is also being done on the problem of measuring heart volume with x-ray cineangiography (Ref. 13). Some of the techniques measure volume from bi-plane films by measuring total heart outline as revealed by the dye. Others measure only maximum heart length and width. Single-plane methods use dye concentration to indicate heart depth. In each case, a computer is used for part or all of the total measurement.

In another application, a computer is used to locate and measure the width of trabecular bone shadows to determine bone mineralization and strength which is reflected in the trabecular pattern (Ref. 14). In this application, the scanned film is first preprocessed by filtering to remove high-frequency noise and background shading. A line-by-line measurement is then made by the computer to determine mean trabecular width, spacing, and frequency. The detection algorithm is the peak-connecting type with minimum and maximum allowable width conditions imposed. Figure 24 shows an example of three lumbar vertebra films with progressive demineralization (*upper*). The bottom row gives a pictorial representation of the computer trabecular shadow detection program. That is, each point of the top picture that the computer decides is part of a trabecular shadow is displayed in the bottom picture as white; the rest is shown black. The principal purpose of this display is to verify the accuracy of the detection process. However, it also represents a type of nonlinear enhancement.

The originator of this technique, Dr. S. David Rockoff of Washington University, St. Louis, initially made these measurements with a mechanical film scanner and an analog computer. Approximately 10 min were required to scan a line of film and to perform the necessary hand calculations. Consequently, it was not practical to take more than a few scans per film. On the other hand, the computer prefiltered and measured 400 scan lines for the films in Fig. 24 in 4 min, or about 0.6 s per line.

VI. Conclusions

The goal of computer enhancement research on x-ray films is to produce medically useful pictures. While the initial results have been interesting and even encouraging, there are several reasons why the goal has not yet been reached.

First of all, image losses from film scanning are still severe although, as previously discussed, they can be decreased substantially with better scanners, particularly with the type that views the original film instead of a reduced version. Without these image losses, an improvement in resolution can undoubtedly be obtained with the computer enhancement. In addition, since the radiologist could screen films more rapidly or more reliably

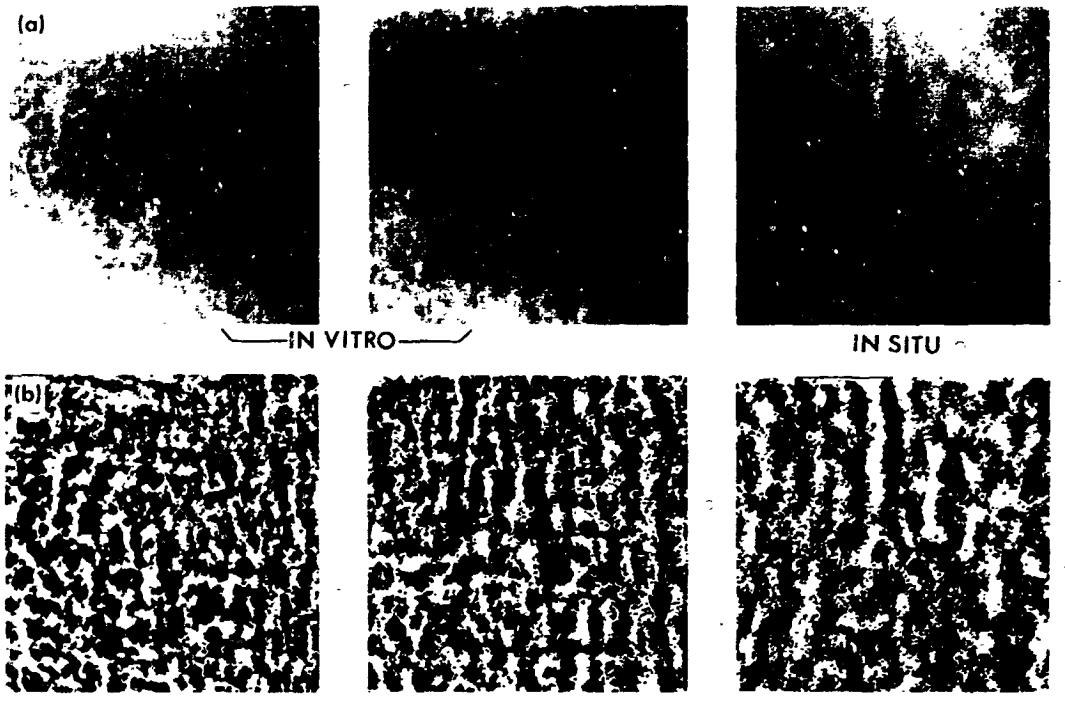

Fig. 24. Lumbar vertebra radiographs and display of trabecular shadow detection: (a) radiographs showing progressive demineralization; (b) pictorial representation of computer program to detect trabecular shadows. Each bottom row point is printed white if corresponding point in top row falls within what computer decides is trabecular shadow, otherwise point is printed black

with an enhanced picture in which selected features are more easily seen than on the original, resolution improvement need not be achieved for enhanced pictures to be useful.

A major obstacle to the application of computer enhancement at the clinical level, aside even from problems of image quality, is processing speed. Actual computer time may be short, varying from 20 or 30 s to 30 min or more, depending on the type of processing and the computer. However, the time required to photographically reduce a film (if that is necessary), scan it, process it in the computer, and then reconstruct the computer output into a photograph is likely to be one or two days under even optimum conditions. The use of computer-controlled film scanners and on-line picture displays from the computer could reduce processing time by a large factor. However, systems of this sort are very expensive.

Perhaps the most medically promising application of computer image processing is in the area of quantitative measurement. The quantitation of trabecular patterns in bone as just described, for example, would be virtually impossible without either a digital or an analog computer. The measurement of heart volume from 100 to 200 frames of x-ray film, which requires two or three weeks a patient when hand methods are used, can be accomplished by computer in an hour or less. It seems likely that applications of this sort will increase rapidly as film scanners become more available.

Appendix

Filter Synthesis and Evaluation

I. Digital Filter Representation in the Frequency Domain

Let x_n, $n = 0, \pm 1, \cdots$, be the discrete series obtained by sampling film every T millimeters and y_n, $n = 0, \pm 1, \cdots$, be the output of a digital filter applied to x_n. If the filter weights are given by $g = (g_{-K}, \cdots, g_K)$, the filter equation is given by

$$y_n = \sum_{k=-K}^{K} g_k x_{n-k}$$

$$n = 0, \pm 1, \cdots \qquad \text{(A-1)}$$

Let the discrete Fourier transform of y_n be defined as

$$Y(f) = \sum_{n=-\infty}^{\infty} y_n e^{-j2\pi fnT} \qquad \text{(A-2)}$$

Substituting Eq. (A-1) into (A-2),

$$Y(f) = \sum_{n=-\infty}^{\infty} \left[\sum_{k=-K}^{K} g_k x_{n-k} \right] e^{-j2\pi fnT}$$

and, after rearranging terms,

$$Y(f) = \sum_{k=-K}^{K} g_k \sum_{n=-\infty}^{\infty} x_{n-k} e^{-j2\pi fnT}$$

After making the change of variable $m = n - k$,

$$Y(f) = \sum_{k=-K}^{K} g_k \sum_{m=-\infty}^{\infty} x_m e^{-j2\pi f(m+k)T}$$

$$= \sum_{k=-K}^{K} g_k e^{-j2\pi fkT} \sum_{m=-\infty}^{\infty} x_m e^{-j2\pi fmT}$$

$$= G(f) \cdot X(f)$$

where we define $g_k = 0$ for $|k| > K$.

Thus the input and output of a digital filter are related in the frequency domain by $G(f)$, the filter transfer function that is found to be the discrete Fourier transform of the filter weights.

II. Calculation of Digital Filter Modulation Transfer Functions

Now consider the MTF of some of the filters discussed earlier in the report. For example, the three-point low-pass filter was defined by the weights,

$$g = (1/3, 1/3, 1/3)$$

Thus,

$$G(f) = \sum_{k=-1}^{1} (1/3)\, e^{-j2\pi fkT}$$

$$= 1/3 + 2/3 \cos(2\pi fT)$$

It is convenient at this point to express the period of the sinusoids in units of samples rather than in millimeters. Thus the unit of frequency becomes cycles per sample and the sample interval T is equal to one as is the sample frequency f_s. Accordingly, a frequency of 0.1 indicates a sinusoid whose period is 10 samples. Conversion of the period to millimeters is accomplished by multiplying by the actual sample spacing.

Thus, with f in cycles per sample, the MTF for the three-point averaging filter becomes

$$G(f) = 1/3 + 2/3 \cos(2\pi f)$$

A plot of $|G(f)|$ is shown in Fig. 5(a).

A basic property of Fourier transforms is that the transform of an even function is real-valued. All filters symmetric about the center weight, therefore, have real-valued transfer functions. Figure 5(b) also shows the MTF for the five-point averaging filter, $g = (1/5, 1/5, 1/5, 1/5, 1/5)$ which is calculated as

$$G(f) = 1/5\,[1 + 2\cos(2\pi f) + 2\cos(4\pi f)]$$

As would be anticipated, the five-point filter falls off faster and thus removes more of the high-frequency signal.

In comparison, the five-point third-degree least-squares filter has MTF

$$G(f) = 1/35\,[17 + 24\cos(2\pi f) - 6\cos(4\pi f)]$$

and as shown in Fig. 6 has a flatter low-frequency response than either of the equal-weight filters.

Earlier it was shown that if g_k are weights for a low-pass filter with MTF $G(f)$, then a high-pass filter is defined as

$$g'_k = \delta(k) - g_k \qquad k = 0, \pm 1, \cdots, \pm K \qquad \text{(A-3)}$$

Further, it was stated that the MTF $G'(f)$ of this filter is given by

$$G'(f) = 1 - G(f)$$

To show this is true, three properties of Fourier transforms are required. Let $F[\,]$ indicate the Fourier transform of the bracketed quantity. Then if $g_1(t)$ and $g_2(t)$ are two spatial functions, the following properties are known:

$$F[g_1(t) + g_2(t)] = F[g_1(t)] + F[g_2(t)]$$

If A = constant, $F[Ag_1(t)] = AF[g_1(t)]$

$F[\delta(t)] = 1$, where $\delta(t)$ is an impulse at the origin

The desired result follows by taking the transform of both sides of Eq. (A-3).

III. Digital Filter Synthesis

Frequently it is desirable to generate a digital filter with a particular given MTF by obtaining the weights from the inverse Fourier transform of the given MTF. Suppose $G^*(f)$ is the given MTF and the sample interval is 1. Then the inverse transform is

$$g_k^* = \int_{f=-\infty}^{\infty} G^*(f) e^{j2\pi fk}\, df \qquad \text{(A-4)}$$

Suppose a truncation function W_k is defined as

$$W_k = 1 \text{ for } -K \leq k \leq K$$

$$= 0 \quad \text{otherwise}$$

and we define a truncated sequence of non-zero weights as

$$g_k = g_k^* W_k \qquad \text{(A-5)}$$

This truncated weight sequence gives an approximation to $G^*(f)$. The MTF is calculated in the usual manner as

$$G(f) = \sum_{k=-K}^{K} g_k e^{-j2\pi fk}$$

Let the mean-square-error difference between $G^*(f)$ and $G(f)$ be defined as

$$\varepsilon = \int_{-0.5}^{0.5} [G(f) - G^*(f)]^2\, df$$

It is known that the filter defined by Eq. (A-4) has the smallest ε among all possible $2K + 1$ weight filters (Ref. 15). However, it is also a fact that a discontinuity in $G^*(f)$ causes overshoot in $G(f)$ which does not decrease to zero as K goes to infinity (Ref. 16).

This overshoot can be avoided by using a different truncation function W_K. For example, the function

$$W_K = 1 - \frac{|k|}{K} \text{ for } -K \leq k \leq K$$

$$= 0 \quad \text{otherwise}$$

when applied to g_k^* produces a filter whose MTF uniformly converges to $G^*(f)$ but at a slower rate than the filter derived from the uniform truncation function (Ref. 17).

There are a considerable number of possible truncation functions whose use depends in general upon the shape of the desired filter and the type of error that can be tolerated.

IV. Two-Dimensional Filter Synthesis

Given the two-dimensional modulation transfer function $G^*(u, v)$, where u and v are spatial frequencies in the horizontal and vertical direction, respectively, the two-dimensional Fourier transform is found as

$$g^*_{k,l} = \int\int G^*(u, v)\, e^{j2\pi(uk+vl)}\, du\, dv$$

$$k = 0, \pm 1, \cdots, l = 0, \pm 1, \cdots \qquad \text{(A-6)}$$

Filter weights $g_{k,l}$ are obtained by truncating $g^*_{k,l}$

That is,

$$g_{k,l} = g^*_{k,l}\, W_{k,l}$$

where

$$W_{k,} = 0 \text{ for } |k| > K, |l| > L$$

The MTF of this filter is obtained as

$$G(u, v) = \sum_{l} \sum_{k} g_{k,l}\, e^{-j2\pi(uk+vl)}$$

Typically, the three-dimensional surface $G^*(u, v)$ is not known except along the horizontal and vertical axes. This necessitates generation of a surface to fit these known functions. A common assumption is that all equi-response contours of $G^*(u, v)$ are ellipses. This assumption, and the condition that the horizontal and vertical responses $G(u, 0)$ and $G(0, v)$ are monotone functions of frequency, allows generation of $G(u, v)$ by iterative solution of the equations

$$u/u_0 + v/v_0 = 1 \text{ and } G(u_0, 0) = G(0, v_0) = G(u, v)$$

In the above, as shown in Fig. A-1, u and v are given, u_0 is chosen arbitrarily, v_0 is determined from the first equation, and then the quantity

$$|G(u_0, 0) - G(0, v_0)|$$

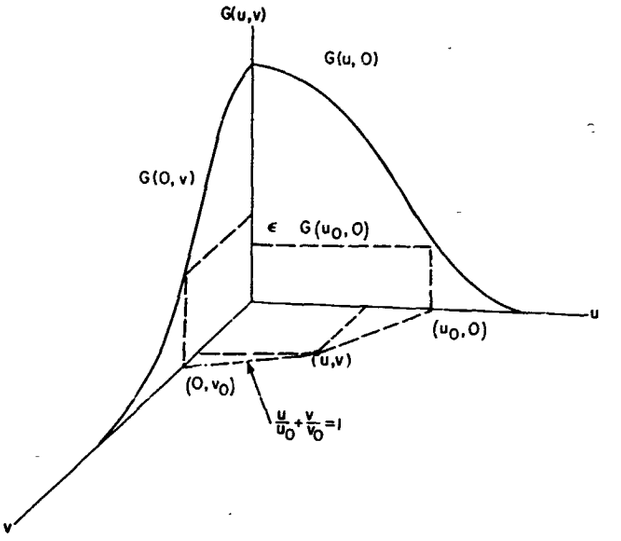

Fig. A-1. Diagram showing method used to obtain surface G(u,v) from projections G(u, 0) and G(0,v); G(u,v) is taken equal to $G(u_0,0)$ when ε is less than some predetermined value

is calculated. If this difference is too large, the procedure is repeated with a new u_0 chosen each time in a direction to decrease the difference.

If $G^*(u, v)$ has circular symmetry, then so does $g^*(u, v)$, and Eq. (A-6) reduces to the one-dimensional Hankel transform. That is, if $q^2 = u^2 + v^2$, $r^2_{k,l} = k^2 + l^2$ and $G^*(u, v) = g^*(q)$, then the Hankel transform to generate filter weights for a symmetric MTF is

$$g(r) = 2\pi \int_{q=0}^{\infty} G^*(q)\, J_0(2\pi qr)\, q\, dq$$

where $J_0(2\pi qr)$ is a zero-order Bessel function of the first kind,

$$J_0(2\pi qr) = 1/2\pi \int_{\phi=0}^{2\pi} e^{j2\pi qr \cos\phi}\, d\phi$$

References

1. Ledley, R. S., et al., *Optical and Electro-Optical Information Processing*, p. 591. The M.I.T. Press, Massachusetts Institute of Technology, Cambridge, 1965.

2. Prewitt, J. M. S., *The Use of Computers in Radiology*, p. A-82. University of Missouri, April 1968.

3. Selzer, R. H., *The Use of Computers in Radiology*, p. A-84. University of Missouri, April 1968.

4. Nathan, R., *Pictorial Pattern Recognition*, p. 239. Thompson Book Company, Washington, D.C., 1968.

5. Rossman, K., "Modulation Transfer Function of Radiographic Systems Using Fluorescent Screens," *J. Opt. Soc. Amer.*, Vol. 52, p. 774, 1962.

6. Rossman, K., and Lubberts, G., "Some Characteristics of the Line Spread-Function and Modulation Transfer Function of Medical Radiographic Films and Screen-Film Systems," *Radiology*, Vol. 86, p. 235, 1966.

7. Morgan, R. H., Bates, L. M., Gopalarao, U. V., Marinaro, A., "The Frequency Response Characteristics of X-ray Films and Screens," *Amer. J. Roentgen.*, Vol. 92, p. 426, 1964.

8. Doi, K., "Optical Transfer Functions of the Focal Spot of X-ray Tubes," *Amer. J. Roentgen.*, Vol. 94, p. 712, 1965.

9. Rossman, K., and Moseley, R. D., "Measurement of the Input to Radiographic Imaging Systems," *Invest. Radiol.* (to be published).

10. Tuddenham, W. J., "Visual Search, Image Organization and Reader Error in Roentgen Diagnosis," *Radiology*, Vol. 78, p. 694, 1962.

11. Hanafee, W., and Stout, P., "Subtraction Technique," *Radiology*, Vol. 70, p. 658, 1962.

12. Becker, H. C., Nettleton, W. J., Meyers, P. H., Sweeney, J. W., Nice, C. M., "Digital Computer Determination of a Medical Diagnostic Index Directly from Chest X-ray Images," *IEEE Trans. Biomed. Engin.*, BME 11, p. 67, 1964.

13. Conference on Measurement of Heart Chamber Volumes and Dimensions, Denver, Colorado, July 24–27, 1967. Summary of proceedings published by the American Heart Association, Inc.

14. Rockoff, S. D., and Selzer, R. H., "Radiographic Trabecular Quantitation of Human Lumbar Vertebrae In Situ," in *Proceedings of the Conference on Progress in Methods of Bone Mineral Measurement, Bethesda, Maryland, February 15–17, 1968.* (Proceedings to be published as a special issue of *Clin. Orthop.*)

15. Ormsby, J., "Design of Numerical Filters With Applications to Missile Data Processing," *J. Soc. Indust. and Appl. Math.*, Vol. 9, p. 440, 1961.

16. Selzer, R. H., "An Evaluation of Three Digital Low-pass Filters," M.S. thesis, University of California, Los Angeles, January 1962.

17. Jenkins, G. M., "General Considerations in the Estimation of Spectra," *Technometrics*, Vol. 3, p. 138, 1961.